

**Electric Transport of a Single Crystal Iron Chalcogenide FeSe  
Superconductor: Evidence of Symmetry Breakdown Nematicity  
and Additional Ultrafast Dirac cone-Like Carriers**

K. K. Huynh<sup>1</sup>, Y. Tanabe<sup>2,\*</sup>, T. Urata<sup>2</sup>, H. Oguro<sup>3</sup>,  
S. Heguri<sup>1</sup>, K. Watanabe<sup>3</sup>, and K. Tanigaki<sup>1,2†</sup>

<sup>1</sup>*WPI-Advanced Institutes of Materials Research, Tohoku University,  
Aoba, Aramaki, Aoba-ku, Sendai, 980-8578, Japan*

<sup>2</sup>*Department of Physics, Graduate School of Science,  
Tohoku University, Aoba, Aramaki,  
Aoba-ku, Sendai, 980-8578, Japan and*

<sup>3</sup>*High Field Laboratory for Superconducting Materials,  
Institute for Materials Research, Tohoku University, Sendai 980-8577, Japan*

(Dated: April 18, 2019)

## Abstract

An SDW antiferromagnetic (SDW-AF) low temperature phase transition is generally observed and the AF spin fluctuations are considered to play an important role for the superconductivity pairing mechanism in FeAs superconductors. However, a similar magnetic phase transition is not observed in FeSe superconductors, which has caused considerable discussion. We report on the intrinsic electronic states of FeSe as elucidated by transport measurements under magnetic fields using a high quality single crystal. A mobility spectrum analysis, an ab initio method that does not make assumptions on the transport parameters in a multicarrier system, provides very important and clear evidence that another hidden order, most likely the symmetry broken from the tetragonal C4 symmetry to the C2 symmetry nematicity associated with the selective d-orbital splitting, exists in the case of superconducting FeSe other than the AF magnetic order spin fluctuations. The intrinsic low temperature phase in FeSe is in the almost compensated semimetallic states but is additionally accompanied by Dirac cone like ultrafast electrons  $\sim 10^4 \text{cm}^2(\text{VS})^{-1}$  as minority carriers.

PACS numbers: 74.70.Xa, 74.25.Dw, 72.15.Gd, 75.47.-m

---

\*Corresponding author: youichi@sspns.phys.tohoku.ac.jp

†Corresponding author: tanigaki@sspns.phys.tohoku.ac.jp

After the discovery of the high temperature superconductivity of  $\text{LaFeAsO}_{1-x}\text{F}_x$  by Kamihara et al. in 2008, a variety of superconducting compounds such as  $\text{FePn}$  ( $\text{Pn} = \text{P}, \text{As}$ ) and  $\text{FeCh}$  ( $\text{Ch} = \text{Se}, \text{Te}$ ) were found and studied [1–7].  $\text{FeSe}$  has the simplest crystal structure among the iron-based superconducting families and is composed of two-dimensional  $\text{FeSe}$  blocks stacked along the  $c$ -axis direction [8, 9], and therefore has become a very important platform for understanding the mechanism of superconductivity as well as the intriguing structural / electronic phase transitions that occur when temperature is lowered. In the  $\text{FeAs}$  superconducting families, a magnetic SDW phase transition generally occurs together with a structural phase transition from tetragonal to orthorhombic. It is generally considered that spin fluctuations of the low temperature antiferromagnetic (AFM) phase play an important role for mediating superconductivity. This is generally denoted as the  $\text{S}\pm$  mechanism [10]. As another candidate for the superconductivity mechanism, the orbital fluctuation in a  $d$ -multiband system has been proposed [11].  $\text{FeSe}$  has been proven to show that no magnetic phase transitions are observed even though a kink in electric conductivity as a function of temperature is observed [12]. Therefore, a surge of interest has arisen to compare the  $\text{FeAs}$  and  $\text{FeSe}$  superconducting families, and hitherto a lot of experiments have been performed so far. However, due to the difficulty in achieving single crystal growth, there have been few experimental reports on the electronic states of  $\text{FeSe}$  [13, 14].

An interesting report regarding the superconductivity has recently been made for  $\text{FeSe}$  by Xue et al., showing that a single layer  $\text{FeSe}$  epitaxially grown on a  $\text{SrTiO}_3$  substrate showed a  $T_c$  much higher than what has been ever seen in the  $\text{Fe}$  superconducting family [15]. However, due to the difficulty in elucidating the intrinsic electronic states of a single layer of  $\text{FeSe}$ , the real nature of superconductivity in  $\text{FeSe}$  is still an important open question. Recently, a method of high quality single crystal growth of 1:1 stoichiometric  $\text{FeSe}$  has been reported [16]. Therefore, it is very important and timely to study the electric transport properties of  $\text{FeSe}$  single crystals.

In this letter, we report on the detailed electronic structure of a  $\text{FeSe}$  bulk single crystal studied by transport measurements under magnetic fields. The experimental data, by employing *ab initio* mobility spectrum analysis without making assumptions on the carrier numbers, clearly demonstrate that the electron and hole pockets with almost equivalent carrier numbers of  $\sim 10^{20} \text{ cm}^{-3}$  are present in the majority of carrier bands, which is consistent with a carrier-compensated semimetallic feature. In addition, we intriguingly find

that another minority band with the carrier number of  $\sim 10^{18} \text{ cm}^{-3}$  is also present. Surprisingly, these minority electron carriers show an ultrafast carrier mobility of  $\sim 10^4 \text{ cm}^2(\text{VS})^{-1}$ . Moreover, both a remarkable reduction in carrier number and an enhancement in carrier mobility were simultaneously observed below 120 K higher than the structural transition temperature. Although no antiferromagnetic (AFM) ordering has been reported in pure FeSe [12], the electronic structure of orthorhombic FeSe single crystal shows a clear change in the electronic structure. The present results provide a very important clue to understand the mechanism of superconductivity and the electronic phase transition of iron-based superconductors.

A single crystal of FeSe was grown by using a KCl and  $\text{AlCl}_3$  flux method [11]. The single crystal of FeSe was characterized by X-ray diffraction (XRD) as well as electrical resistivity measurements [See Supplementary Information]. The (0 0 1) reflections of the FeSe single crystal is consistent with that of tetragonal structure of FeSe [8, 9]. A temperature dependence of electrical resistivity  $\rho$  showed a kink at around 90 K associated with the structure phase transition, being almost consistent with previous reports [8]. Electrical transport measurements were carried out using a four probe method under magnetic fields up to 15 T in the temperature range between 12 and 200 K.

Figure 1(a) shows a typical temperature dependence of the resistivity ( $\rho(T)$ ) observed in our FeSe single crystals. A clear kink in  $\rho(T)$  is always observed at the structural transition  $T^* = 90 \text{ K}$ , hinting that an electronic structure transition takes place. Interestingly, the change in electronic states indicated by the kink became clear when we carried out the conductivity experiments under a magnetic field ( $B$ ) (magnetoresistance MR) and the Hall resistivity ( $R_H$ ) above and below  $T^*$ , as shown in figures 1(b) and 1(c). Below the  $T^* = 90 \text{ K}$  [See Supplementary Information],  $(R_{xx}(B))/R(0)$  increased with a decrease in  $T$  and became 300 % at 12 K under 9 T, while it was very small above  $T^*$ . The value of  $\rho_{yx}$  developed non-linearly below  $T^*$  and a clear sign change in  $\rho_{yx}$  were confirmed at low  $T$ 's [17]. These abrupt changes in the  $B$ -dependence of the magneto-transport properties unambiguously suggest a drastic reconstruction of the Fermi surfaces across the transition at  $T^*$ . From the view point of the semiclassical theory of transport, such a large enhancement of MR can be directly linked to a big jump in the carrier mobility, whereas a sign change of  $R_H$  can appear only in the case where a large change in mobility takes place between electron-like and hole-like carriers. As we shall see in the analysis below, these curious

behaviors of the transport properties are indeed associated with a very unique evolution of the electronic structure as a function of temperature.

Because the current material is a d-multiband semimetal, it is generally difficult to have a clear understanding of the magneto-transport properties due to the mixing of many possible Fermi pockets. A conventional method in this situation is to construct a model by hypothesizing the number of carrier types, where each is characterized by two parameters: carrier density and mobility. These can be estimated by applying the least-square fitting technique to the  $B$ -dependences of  $R_H$  or MR. The results obtained in such an analysis, however, is highly dependent on the preliminary assumption about the number of pockets. In order to avoid any ambiguities for making reasonable interpretations, we employed here the mobility spectrum analysis to understand the low temperature magneto-transport (see SI for more details). Instead of making assumptions on the number of Fermi pockets, we evaluated the distribution of the carrier numbers in the mobility spectrum space [18–20]. In other words, the transverse and the longitudinal conductivities under  $B$  can be described by the distributions  $s^n$  and  $s^p$ ,

$$X(B) = \int_0^\infty \frac{s^n(\mu)}{1 + \mu^2 B^2} + \int_0^\infty \frac{s^p(\mu)}{1 + \mu^2 B^2} = X^n(B) + X^p(B), \quad (1)$$

$$Y(B) = \int_0^\infty \frac{\mu s^n(\mu)}{1 + \mu^2 B^2} + \int_0^\infty \frac{\mu s^p(\mu)}{1 + \mu^2 B^2} = Y^n(B) + Y^p(B). \quad (2)$$

Here  $n$  and  $p$  represent the electron and the hole carriers, respectively and  $\mu$  is the carrier mobility. A set of  $[X^k(B), Y^k(B)]$  denotes the partial longitudinal and transverse conductivities for electron ( $k = n$ ) or hole ( $k = p$ ) carriers.

The  $\mu$ -spectrum  $s^k(\mu)$  was successfully evaluated for electron-like and hole-like carriers using the partial conductivities  $[X^n(B), Y^n(B)]$  and  $[X^p(B), Y^p(B)]$  as shown in Figs. 2 [See Supplementary Information for the details of calculations]. A nearly single-peak structure centered at around  $\mu \sim 1000 \text{ cm}^2(\text{VS})^{-1}$  with the carrier number  $P \sim 10^{20} \text{ cm}^{-3}$  was found in the hole-like carrier region. In contrast, a somewhat broad, double peak structure was deduced in the electron-like carrier region. The value of  $\sigma_0 s^n(\mu)/e\mu$  showed that the 1st peak is at around  $\mu \sim 1000 \text{ cm}^2(\text{VS})^{-1}$  with the carrier number  $N \sim 9 \times 10^{19} \text{ cm}^{-3}$ . This estimated carrier concentration is comparable with  $\sigma_0 s^p(\mu)/e\mu$  for hole like carriers in the mobility spectrum space, which is indicative of a semimetallic feature of the FeAs single crystal (the first peak deduced from the transport analysis in the electron region can be assigned to the main electron-like carriers.). Taking these experimental facts into account,

the stoichiometric FeSe single crystal is a carrier compensated semimetal and an almost equivalent amount of carriers with similar mobilities exist in both hole and electron regions. Intriguingly, a broad peak structure (the second peak) was observed with the carrier number of  $N \sim 10^{18} \text{ cm}^{-3}$  in the electron region. Since high mobility carriers could be dominant in  $X(B)$  and  $Y(B)$  in the semiclassical transport theory, these minority electron-like carriers with  $\mu \sim 10000 \text{ cm}^2(\text{VS})^{-1}$  should play a significant role in the electrical transport of FeSe at low  $B$ 's even when its carrier number is much smaller than that of the majority electron carriers.

An important result of the  $\mu$ -spectrum is the confirmation of the compensation in carrier number between the hole-like and the electron-like pockets in the material. Moreover, density functional theory (DFT) calculations have shown that the tetragonal phase of FeSe exhibits a semimetal-like FS [21]. These allow us to extend our analysis to higher temperatures in the framework of a semimetallic approximation, i.e.  $N = P$ , and consequently study the changes of the electronic structures in terms of the transport parameters. At high  $T$ 's, since  $(R_{xx}(B))/R(0)$  and the non-linear  $\rho_{yx}$  were significantly suppressed, the mobility spectrum analysis could not monitor the whole electronic structure under the normal magnetic fields of the present experiments. In a two-carrier type semiclassical approximation in the low- $B$  limit, the zero-field resistivity( $\rho_{xx}(0)$ ),  $(R_{xx}(B))/R(0)$ , and  $\rho_{yx}$  were described as

$$\rho_{xx}(0) = \frac{1}{e(n_e\mu_e + n_h\mu_h)}, \quad (3)$$

$$R_{xx}(B)/R(0) = \frac{n_en_h\mu_e\mu_h(\mu_e + \mu_h)^2 B^2}{(n_e\mu_e + n_h\mu_h)^2}, \quad (4)$$

$$\rho_{yx} = \frac{(-n_e\mu_e^2 + n_h\mu_h^2)B}{e(n_e\mu_e + n_h\mu_h)^2} \dots \quad (5)$$

Here  $n_e$  and  $n_h$  are the carrier numbers and  $\mu_h$  and  $\mu_e$  are the mobilities of electrons and holes. Employing Eqs. (3) - (5) under the condition of  $n_e = n_h$ , the transport parameters could be evaluated analytically. The deduced carrier numbers and their mobilities of  $N = P$ ,  $\mu_e$  and  $\mu_h$  are displayed in Figs. 3 (a) and (b). Below 120 K,  $n$  gradually decreased with a decrease in  $T$  and dropped below  $T^*$ , and at low- $T$ 's  $n$  became  $\sim 9 \times 10^{19} \text{ cm}^{-3}$ . Compared with the carrier numbers ( $n_{MS}^k$ ,  $k = n, p$ ) estimated from the mobility spectrum analysis,  $n_{MS}^n \sim 9 \times 10^{19} \text{ cm}^{-3}$  and  $n_{MS}^p \sim 1 \times 10^{20} \text{ cm}^{-3}$  are reasonable. Therefore, 80 - 90 % of the carriers were killed at low- $T$ 's. Both  $\mu_e$  and  $\mu_h$  gradually increased with a decrease in  $T$  below 120 K.

From the mobility spectrum analysis, the low temperature electronic structure of FeSe was successfully investigated. The hole-like carriers can be explained in terms of almost uniform single-peak mobilities in the mobility spectrum space. On the other hand, the electron-like carriers could be divided in two components in the mobility space. The first peak with low mobility of  $\mu \sim 1000 \text{ cm}^2(\text{VS})^{-1}$  is almost compensated with that of the hole-like carriers. The second peak with the much higher mobility of  $\mu \sim 10000 \text{ cm}^2(\text{VS})^{-1}$  plays a key role in the electrical transport under low  $B$ . In the collinear-type AFM phase at low  $T$ 's in the parent compounds of iron-based superconducting families, the electronic bands composed of both minority Dirac cone carriers with high mobility and majority normal carriers accommodated in the almost compensated parabolic bands were reported [20, 22–24]. Because no AFM phase was reported in FeSe under ambient pressure conditions [12], the evolution of the electronic states as a function of  $T$  in FeSe is indeed intriguing when compared with the other iron based superconducting families.

In the low temperature orthogonal phase, the electronic structure of FeSe is represented as an almost compensated semimetal state with ultrafast minority electron-like carriers. Moreover, since the reduction in the carrier number as well as the enhancement in the carrier mobility was confirmed below around 120 K (importantly higher than the structural phase transition temperature being indicative of the occurrence of another hidden order), the electronic structure of FeSe should unambiguously change at low  $T$ 's. The band calculations predicted that the electron and the hole compensation takes place in the high temperature tetragonal phase with carrier numbers of  $N, P = 2.91 \times 10^{21} \text{ cm}^{-3}$  as well as in the low temperature collinear-type AFM phase with the carrier number of  $N = 2.7 \times 10^{20} \text{ cm}^{-3}$  ( $P = 1.8 \times 10^{20} \text{ cm}^{-3}$ ) [25]. However, no AFM phase was reported in the low temperature orthogonal phase in FeSe. Recent ARPES experiments in single crystal FeSe clearly displayed the energy band splitting associated with the orbitals selectively involved in the band at low temperatures, which is consistent with the interpretation of the electronically driven nematicity [26]. In this case, the lift-off of the energy bands could reduce not only the carrier number but also the electron-electron scattering in the electron and the hole FSs. Consequently, both suppression in number and enhancement in mobility of carriers starting at a certain temperature above  $T^*$  could reasonably be understood in terms of the electronically nematic ordering. In Fe based superconductors, the pairing mechanism of the superconductivity and the origin of the electronic nematicity have been discussed in terms

of magnetic and orbital fluctuations [10, 11, 27]. Our present results indicate that the intrinsic scenario for the superconducting mechanism of FeSe-based superconductors involves the mediation via the pure orbital fluctuations, which is in strong contrast with other FeAs superconductors.

Finally, we would like to discuss the origin of the ultrafast minority electron-like carriers observed in the  $\mu$ -spectrum. Such high  $\mu$  carriers can originate from the enhancement of the anisotropic FSs due to orbital splitting. Since  $\mu$  is directly proportional to the Fermi velocity and the effective mass, this anisotropy may exert a strong influence on the k-position of FS's, giving a broad distribution of the mobility spectrum. Another scenario is that a Dirac cone is created due to the splitting of energy bands. In the latter case, the orbital splitting of energy band at low T's can lift up a crossing between the two bands with distinctly different orbital characters ( $d_{xy}$  and  $d_{yz}$ ) in the vicinity of the Fermi energy [28]. Since the Dirac cones originate from band crossings in a three-dimensional system, FeSe can be an intriguing platform to study such unique quantum states, which have recently been discussed in the Ba(FeAs)<sub>2</sub>, Na<sub>3</sub>Bi and Cd<sub>3</sub>As<sub>2</sub> [24, 29–32].

We investigated the electronic structures of FeSe using a high quality single crystal synthesized by a recently reported new method, with analyses in the framework of a semiclassical transport theory. The mobility spectrum employed as a powerful new analytical method clearly demonstrated that the electronic structure in the low temperature orthogonal phase can be described as an almost compensated semimetal involving a minority band with ultrafast carrier mobility. The ultrafast electron-like carriers could be interpreted as originating either from the Dirac cone or large anisotropy of FS's. Moreover, a remarkable reduction in carrier number and an enhancement in carrier mobility were simultaneously observed below 120 K higher than  $T^*$ . In comparison with the ARPES experiments [26], this significant change in the electronic structure was reasonably understood in terms of the development of electronically driven nematic ordering.

### Acknowledgements

We are grateful to Quynh T. N. Phan to support constructions of electrical transport measurement system under high magnetic fields and for K. Saito (Common Equipment Unit of Advanced Institute for Materials Research, Tohoku University) to support the XRD

measurements The research was partially supported by Grant-in-Aid for Young Scientists (B) (23740251) and the Joint Studies Program (2013) of the Institute for Molecular Science

- 
- [1] Y. Kamihara, H. Hiramatsu, M. Hirano, R. Kawamura, H. Yanagi, T. Kamiya, H. Hosono, J. Am. Chem. Soc. **128**, 10012 (2006)./Y. Kamihara, T. Watanabe, M. Hirano, H. Hosono, J. Am. Chem. Soc. **130**, 3296-3297 (2008).
- [2] M. Rotter, M. Tegel, and D. Johrendt, Phys. Rev. Lett. **101**, 107006 (2008).
- [3] X. C. Wang, Q.Q. Liu, Y.X. Lv, W.B. Gao, L. X. Yang, R. C. Yu, F. Y. Li, C. Q. Jin, Solid State Commun. **148**, 538-540 (2008).
- [4] M. Rotter, M. Pangerl, M. Tegel, and D. Johrendt, Angew. Chem., Int. Ed. **47**, 7949 (2008).
- [5] J. Guo, S. Jin, G. Wang, S. Wang, K. Zhu, T. Zhou, M. He, and X. Chen, Phys. Rev. B **82**, 180520(R) (2010).
- [6] S. Kakiya, K. Kudo, Y. Nishikubo, K. Oku, E. Nishibori, H. Sawa, T. Yamamoto, T. Nozaka, and M. Nohara, J. Phys. Soc. Jpn. **80**, 093704 (2011).
- [7] H. Ogino, Y. Matsumura, Y. Katsura, K. Ushiyama, S. Horii, K. Kishio and J. Shimoyama, Supercond. Sci. Technol. **22**, 075008 (2009).
- [8] F. C. Hsu, J. Y. Luo, K. W. Yeh, T. K. Chen, T. W. Huang, P. W. Wu, Y. C. Lee, Y. L. Huang, Y. Y. Chu, D. C. Yan, and M. K. Wu, Proc. Nat. Aca. Sci. **105**, 14262-14264 (2008).
- [9] S. Margadonna, Y. Takabayashi, M. T. McDonald, K. Kasperkiewicz, Y. Mizuguchi, Y. Takano, A. N. Fitch, D. E. Suard, K. and Prassides, Chem. Commun. **43**, 5607-5609 (2008).
- [10] I. I. Mazin, D. J. Singh, M. D. Johannes, M. H. Du, Phys. Rev. Lett. **101**, 057003 (2008). / K. Kuroki, S. Onari, R. Arita, H. Usui, Y. Tanaka, H. Kontani, and H. Aoki, Phys. Rev. Lett. **101**, 087004 (2008). / F. Wang, H. Zhai, Y. Ran, A. Vishwanath, and D. H. Lee, Phys.Rev. Lett. **102**, 047005 (2009). / V. Cvetkovic, Z. Tesanovic, Europhys. Lett. **85**, 37002 (2009).
- [11] H. Kontani, and S. Onari, Phys. Rev. Lett. **104**, 157001 (2010).
- [12] R. Khasanov, K. Conder, E. Pomjakushina, A. Amato, C. Baines, Z. Bukowski, J. Karpinski, S. Katrych, H.-H. Klauss, H. Luetkens, A. Shengelaya and N. D. Zhigadlo, Phys. Rev. B **78**, 220510(R) (2008).
- [13] C. L. Song, Y. L. Wang, P. Cheng, Y. P. Jiang, W. Li, T. Zhang, Z. Li, K. He, L. Wang, J.

- F. Jia, H. H. Hung, C. Wu, X. Ma, X. Chen, Q. X. Xue, *Science* **332**, 1410 (2011).
- [14] J. Maletz, V. B. Zabolotnyy, D. V. Evtushinsky, S. Thirupathiah, A. U. B. Wolter, L. Harnagea, A. N. Yaresko, A. N. Vasiliev, D. A. Chareev, E. D. L. Rienks, B. Buchner and S. V. Borisenko, arxiv1307.1280.
- [15] Q. Y. Wang, L. Zhi, W. H. Zhang, Z. C. Zhang, J. S. Zhang, W. Li, H. Ding, Y. B. Ou, P. Deng, K. Chang, J. Wen, C. L. Song, K. He, J. F. Jia, S. H. Ji, Y. Y. Wang, L. L. Wang, X. Chen, X. C. Ma, Q. K. Xue, *Chin. Phys. Lett.* **29**, 037402 (2012).
- [16] A. E. Bohmer, F. Hardy, F. Eilers, D. Ernst, P. Adelman, P. Schweiss, T. Wolf and C. Meingast, *Phys. Phys. Rev. B* **87**, 180505(R) (2013).
- [17] H. Lei, D. Graf, R. Hu, H. Ryu, E. S. Choi, S. W. Tozer, and C. Petrovic, *Phys. Rev. B* **85**, 094515 (2012).
- [18] J. McClure, *Phys. Rev.* **112**, 715 (1958).
- [19] W. Beck, J. Anderson, *J. of Appl. Phys.* **62**, 541 (1987).
- [20] K. K. Huynh, Y. Tanabe, T. Urata, S. Heguri, K. Tanigaki, T. Kida, M. Hagiwara, arxiv1403.6992.
- [21] A. Subedi, L. Zhang, D. J. Singh, M. H. and Du, *Phys. Rev. B* **78**, 134514 (2008).
- [22] P. Richard, K. Nakayama, T. Sato, M. Neupane, Y.-M. Xu, J. H. Bowen, G. F. Chen, J. L. Luo, N. L. Wang, X. Dai, Z. Fang, H. Ding, and T. Takahashi, *Phys. Rev. Lett.* **104**, 137001 (2010).
- [23] Y. Zhang, C. He, Z. R. Ye, J. Jiang, F. Chen, M. Xu, Q. Q. Ge, B. P. Xie, J. Wei, M. Aeschlimann, X. Y. Cui, M. Shi, J. P. Hu, and D. L. Feng, *Phys. Rev. B* **85**, 085121 (2012).
- [24] Y. Ran, F. Wang, H. Zhai, A. Vishwanath, D. Lee, *Phys. Rev. B* **79**, 014505 (2009)./ T. Morinari, E. Kaneshita, T. Tohyama, *Phys. Rev. Lett.* **105**, 037203 (2010)./ Z. P. Yin, K. Haule, G. Kotliar, *Nat. Phys.* **7**, 294 (2011).
- [25] F. Ma, W. Ji, J. Hu, Z. Y. Lu, and T. Xiang, *Phys. Rev. Lett.* **102**, 177003 (2009).
- [26] K. Nakayama, Y. Miyata, G. N. Phan, T. Sato, Y. Tanabe, T. Urata, K. Tanigaki, and T. Takahashi, arxiv1404.0857./ T. Shimojima, JPS annual meeting 2014.
- [27] R. M. Fernandes, A. V. Chubukov, and J. Schmalian, *Nat. Phys.* **10**, 97 (2014).
- [28] K. Nakayama, private communications.
- [29] N. Harrison, S. E. and Sebastian, *Phys. Rev. B* **80**, 224512 (2009)./ K. K. Huynh, Y. Tanabe, K. Tanigaki, *Phys. Rev. Lett.* **106**, 217004 (2011).

- [30] S. M. Young, S. Zaheer, J. C. Teo, C. L. Kane, E. J. Mele, and A. M. Rappe, *Phys. Rev. Lett.* **108**, 140405 (2012).
- [31] Z. Wang, Y. Sun, X.-Q. Chen, C. Franchini, G. Xu, H. Weng, X. Dai, and Z. Fang, *Phys. Rev. B* **85**, 195320 (2012). / Z. K. Liu, B. Zhou, Y. Zhang, Z. J. Wang, H. M. Weng, D. Prabhakaran, S.-K. Mo, Z. X. Shen, Z. Fang, X. Dai, Z. Hussain, Y. L. Chen, *Science* **343**, 864 (2014).
- [32] M. Neupane, S.-Y. Xu, R. Sankar, N. Alidoust, G. Bian, C. Liu, I. Belopolski, T.-R. Chang, H.-T. Jeng, H. Lin, A. Bansil, F. Chou, and M. Z. Hasan, arXiv:1309.7892. / Z. Wang, H. Weng, Q. Wu, X. Dai, and Z. Fang, *Phys. Rev. B* **88**, 125427 (2013).

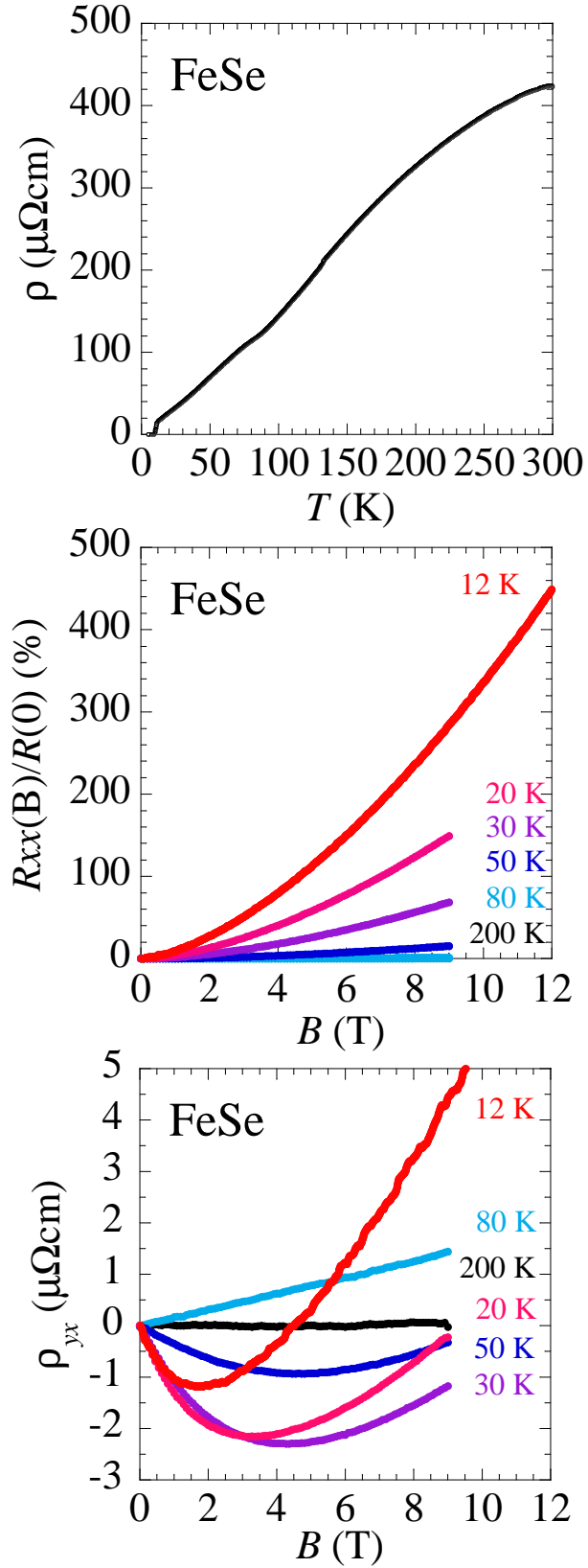


FIG. 1: (color online)(a) Temperature dependence of the resistivity of FeSe single crystal. (b), (c) Temperature evolution of electronic structures of FeSe and magnetic field dependence of magnetoresistance ( $(R_{xx}(B))/R(0)$ ) and Hall resistivity ( $\rho_{yx}$ ) at various temperatures between 12 and 200 K.

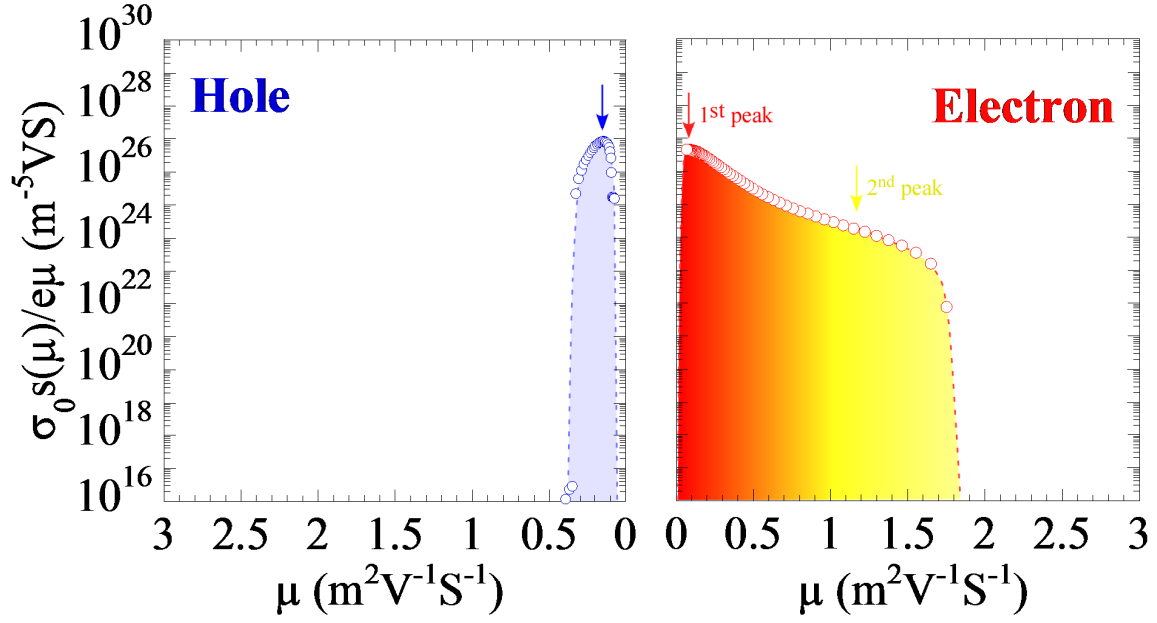


FIG. 2: (color online) Mobility spectra of electron-like and hole-like carriers for FeSe in the low temperature orthogonal phase displayed on a semi-logarithmic scale.

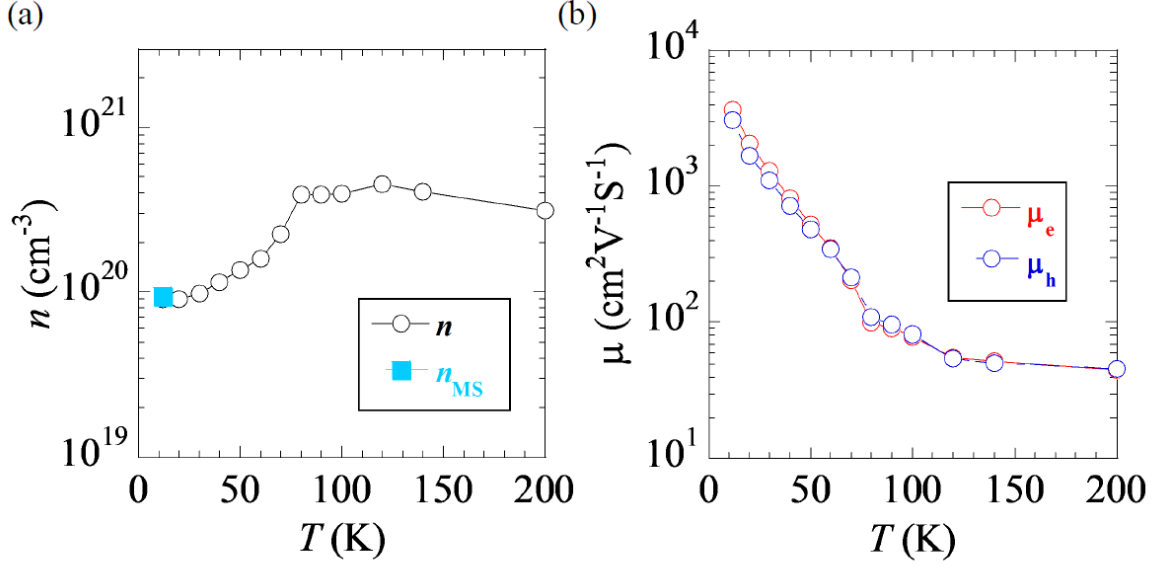


FIG. 3: (color online) (a), (b) Temperature dependences of carrier numbers ( $n$ ) and electron (hole) mobility  $\mu_e$  ( $\mu_h$ ) derived using a two carrier-type semiclassical model in the low  $B$  limit, assuming an electron and hole compensated electronic structure.  $n_{MS}$  is the averaged carrier number of electron-like and hole-like carriers ( $n_{MS}^k, k = n, p$ ) estimated from the mobility spectra.